Superconductive and normal-state transport properties of epitaxial $YBa_2(Cu_{1-x}Ni_x)_3O_7$ films

M. Speckmann, Th. Kluge, C. Tomé-Rosa, Th. Becherer, and H. Adrian
Institut für Festkörperphysik, Technische Hochschule Darmstadt, Hochschulstrasse 8, D-6100 Darmstadt, Germany
(Received 14 January 1993)

Ni-doped epitaxial thin $YBa_2(Cu_{1-x}Ni_x)_3O_{7-\delta}$ films have been prepared by high-oxygen-pressure dc sputtering from stoichiometric targets on $SrTiO_3$ substrates. Structural properties of these *c*-axis-oriented films were not affected by Ni doping up to $x = 15\%$. Inductively measured transition temperatures show a decrease with a rate of -4.5 K/(at. % Ni) for Ni concentrations up to $x = 4\%$. For higher Ni contents the T_c-depression rate changes to -1.5 K/(at. % Ni). A change in slope is also detectable in the dependence of the resistivity on Ni concentration. These results can be explained in a model based on a concentration-dependent site preference of the Ni atoms. The activation energy for vortex creep (extracted from resistive transitions) and the critical-current density show the pinning effectiveness of the dopant. Scaling laws for the pinning-force density have also been studied. The Hall concentration n_H shows a slight increase for small x and a decrease for higher values. The slope dn_H/dT is also lowered for increasing Ni content. Furthermore, the mobility and the Hall angle of the $YBa_2(Cu_{1-x}Ni_x)_3O_{7-\delta}$ films were deduced from experimental data.

I. INTRODUCTION

The change of normal and superconductive transport properties due to the substitution of copper in $YBa_2Cu_3O_{7-\delta}$ by other 3*d* transition metals (e.g., Ni) is of particular interest in understanding parameters essential for superconductivity. From experiments on bulk material it is already known that Ni leads to a decrease of the superconducting critical temperature T_c. The experimental results on $YBa_2(Cu_{1-x}Ni_x)_3O_{7-\delta}$ bulk samples reported so far give evidence for Ni substituting Cu in the CuO_2-plane sites [Cu(2)].[1–3] But there are also reports deducing the substitution in both the CuO_2-plane sites and the CuO sites [Cu(1)].[4–6] Varying results are also reported on the strength of T_c depression reaching from -3.6 (K/at. % Ni) (Ref. 7) up to -10.5 (K/at. % Ni),[6] even if eventually observed impurities due to incomplete solubility are corrected. Because of the difficulties in obtaining high-quality doped single crystals with well-defined Ni content, most groups investigated only few doping levels (especially below $x = 1\%$) or narrow doping intervals in bulk material, giving only a crude overview of the change in physical properties. Moreover, measurements of the intrinsic critical-current density in polycrystalline bulk material are ruled out by grain-boundary effects.

Epitaxial thin films are suited ideally to perform direct j_c and Hall-effect measurements, if they are patterned in appropriate structures. This paper presents a detailed, systematic study of the influence of Ni substitution on the normal-state transport and superconducting properties of $YBa_2(Cu_{1-x}Ni_x)_3O_{7-\delta}$. To this purpose, we prepared epitaxially grown high-quality films on $SrTiO_3$ substrates for ten different Ni concentrations in the range of $0 \leq x \leq 0.15$. All films were characterized by x-ray diffraction and ac susceptibility. After patterning, electrical resistivity and Hall measurements were performed. In order to study the effect of Ni impurities on vortex pinning, we measured superconducting critical transport currents $j_c^{ab}(B,T)$ and resistive transitions in high magnetic fields.

II. EXPERIMENTAL DETAILS

For the preparation of $YBa_2(Cu_{1-x}Ni_x)_3O_{7-\delta}$ sputter targets (diameter 32 mm), we first prepared pure $YBa_2Cu_3O_{7-\delta}$-powder and $YBa_2(Cu_{0.8}Ni_{0.2})_3O_{7-\delta}$-powder by solid-state reaction using stoichiometric amounts of Y_2O_3, $BaCO_3$, CuO, and NiO powders as described elsewhere.[8] These two starting materials were thoroughly mixed to obtain a homogeneous and reliable distribution of the Ni atoms in the intended concentration. The targets were bonded to a planar, water-cooled cathode in a noncommercial sputtering system. The *c*-axis-oriented films were prepared by sputtering onto (100)-oriented $SrTiO_3$ substrates mounted on a Pt ribbon, which was resistively heated to $T_{Pt} = 920\,^{\circ}C$, using 3.5 hPa pure oxygen as process gas. Deposition was terminated after 2 h, leading to a film thickness of 1500–2000 Å measured by optical and mechanical methods with an accuracy of about 10%. In order to increase the oxygen content, the films were annealed *in situ* for 30 min at $T_{Pt} = 570\,^{\circ}C$ after venting the sputter chamber with 1000 hPa oxygen. Then they were cooled down to room temperature with a rate of -20 K/min.

X-ray-diffraction and ac-susceptibility measurements to determine T_c were carried out routinely. In order to further characterize the samples, sputtered neutrals mass spectrometry (SNMS) and scanning-electron-microscopy (SEM) measurements were performed for at least one film of every concentration. Silver pads were evaporated on the films and annealed to achieve contact resistances of

the order of 10 mΩ, which are able to carry currents up to 1 A. After oxygen recharging, the samples were patterned wet chemically using highly diluted H_3PO_4 for etching. The patterned structure allows four-probe measurements of the Hall effect and the resistivity on a 200-μm-wide and 1.8-mm-long strip. The critical-current density j_c was measured in dc technique using a 1-μV criterion over a 100-μm-long and 10-μm-wide microbridge.

Hall measurements were performed in magnetic fields parallel to the c axis of the films. Since the Hall voltage U_H was found to increase linearly with the magnetic field, we measured the temperature dependence of the Hall effect by monitoring U_H in a constant magnetic field of 5 T and sweeping the temperature from 300 K down to T_c. Thermal voltages were eliminated by measuring the voltage drop for both current directions. The resistive contribution was substracted by a second run in opposite magnetic field.

Furthermore, the temperature dependence of the electrical resistivity, $\rho(T)$, was measured for all concentrations. For the determination of the activation energy for vortex creep, we measured the resistive transitions to superconductivity in a range of $T_{c0} \leq T \leq 100$ K and in magnetic fields up to 12 T parallel to the c axis of the films.

III. T_c AND RESISTIVITY MEASUREMENTS

X-ray diffraction (XRD) using Bragg-Brentano geometry showed only (00ℓ) peaks, and rocking curves of the (005) peak indicated no broadening of the full width at half maximum (FWHM) value which is typically 0.4°. This indicates the c-axis orientation and the epitaxial growth of the films. XRD, SNMS, and microprobe measurements revealed no indications of impurity phases or deviations from stoichiometric composition up to the highest Ni concentration $x = 15\%$. SEM showed smooth surfaces. The midpoints of the inductive transitions are plotted in Fig. 1. The critical temperature decreases with increasing Ni content at a rate of -4.5 K/at. % Ni up to $x \approx 4\%$. This T_c depression is lowered to -1.5 K/at. % Ni at higher concentrations. Whereas the transition widths (90% signal and 10% signal) are not strongly affected having values $\Delta T_c \leq 1$ K up to $x = 4\%$ and less than 5 K at $x = 15\%$. Error bars indicate twice the standard deviation σ from the mean value of T_c based on the number of films indicated for each concentration.

Considering only the inductive data, two explanations of the change in slope dT_c/dx are possible, namely, first, incomplete solubility of Ni at higher x values and, second, change in site preference of Ni. Since no impurities are discernible and measurements of resistivity show also a change in the slope of $d\rho/dx$ at $x \approx 4\%$, we are convinced that the site preference of Ni changes. Welp *et al.*[9] showed that the conductivity of $YBa_2Cu_3O_{7-\delta}$ could be understood by considering a parallel circuit of copper chains and planes as

$$\rho = \frac{\rho_C \rho_P}{\rho_C + \rho_P}. \tag{1}$$

A fit of this model to our experimental data using a linear increase of resistivity of chains and planes with increasing Ni content is shown in Fig. 2 for the resistivity $\rho(300\,\mathrm{K})$. In this fit we assume that, up to 4%, only CuO_2-plane sites were occupied by Ni, while at higher x values the substitution also takes place at the CuO-chain sites, leading to partial resistivities of chains and planes as

$$\rho_P = m_P(x - C_C) + \rho_{P0}, \tag{2}$$

$$\tilde{\rho}_C = m_C C_C + \tilde{\rho}_{C0}. \tag{3}$$

Since our films are twinned, we introduce a chain resistivity $\tilde{\rho}_C$, which is related to the chain resistivity ρ_C by $\tilde{\rho}_C = \sqrt{2}\rho_C$ due to geometrical reasons. Contributions of the twin boundaries to the resistivity are neglected. C_C is the Ni concentration on the chain sites. It is calculated as the fraction β of Ni that occupies the chain sites for Ni concentrations higher than 4%:

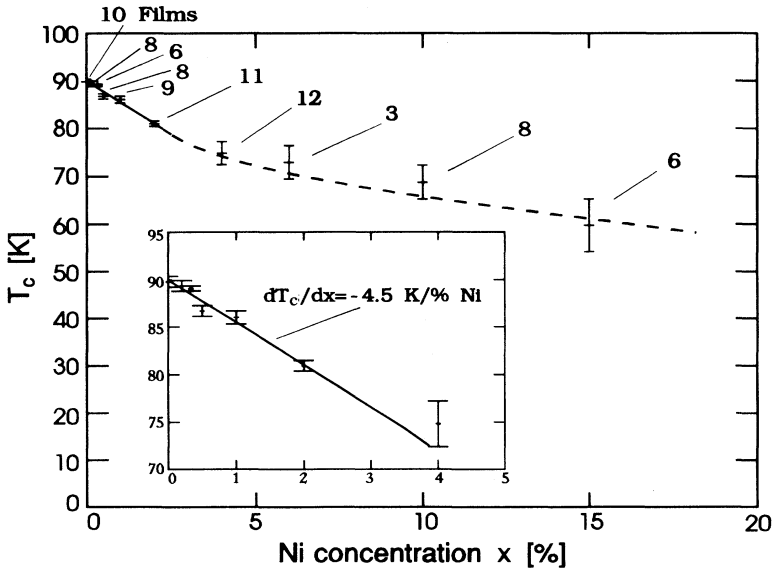

FIG. 1. Influence of the Ni concentration x on the inductively measured transition temperatures $T_c(x)$. The T_c depression is -4.5 K/at. % Ni for $x \lesssim 4\%$, and changes to -1.5 K/at. % Ni for higher Ni content. The error bars indicate twice the standard deviation σ from the mean value of all the films.

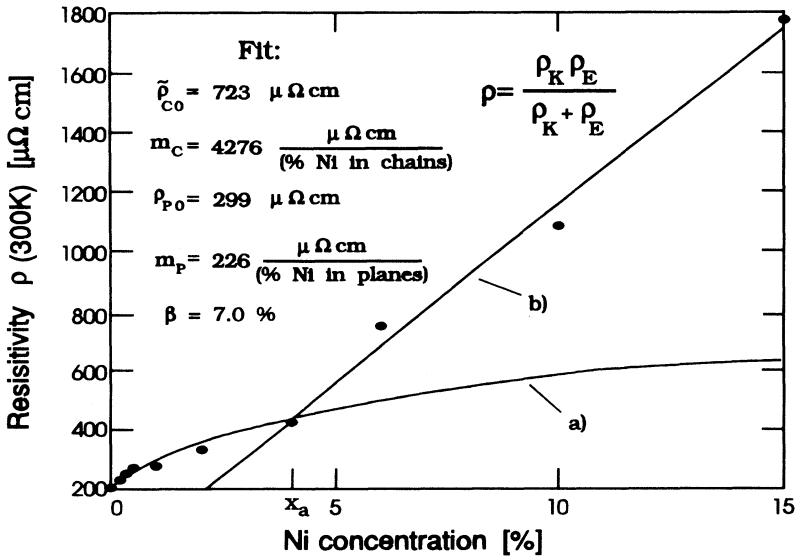

FIG. 2. Resistivity at $T = 300\,\mathrm{K}$ dependent on Ni concentration. The solid line is a fit assuming that for $x \geq 4\%$ also the CuO-chain sites are substituted by Ni. Details are given in the text.

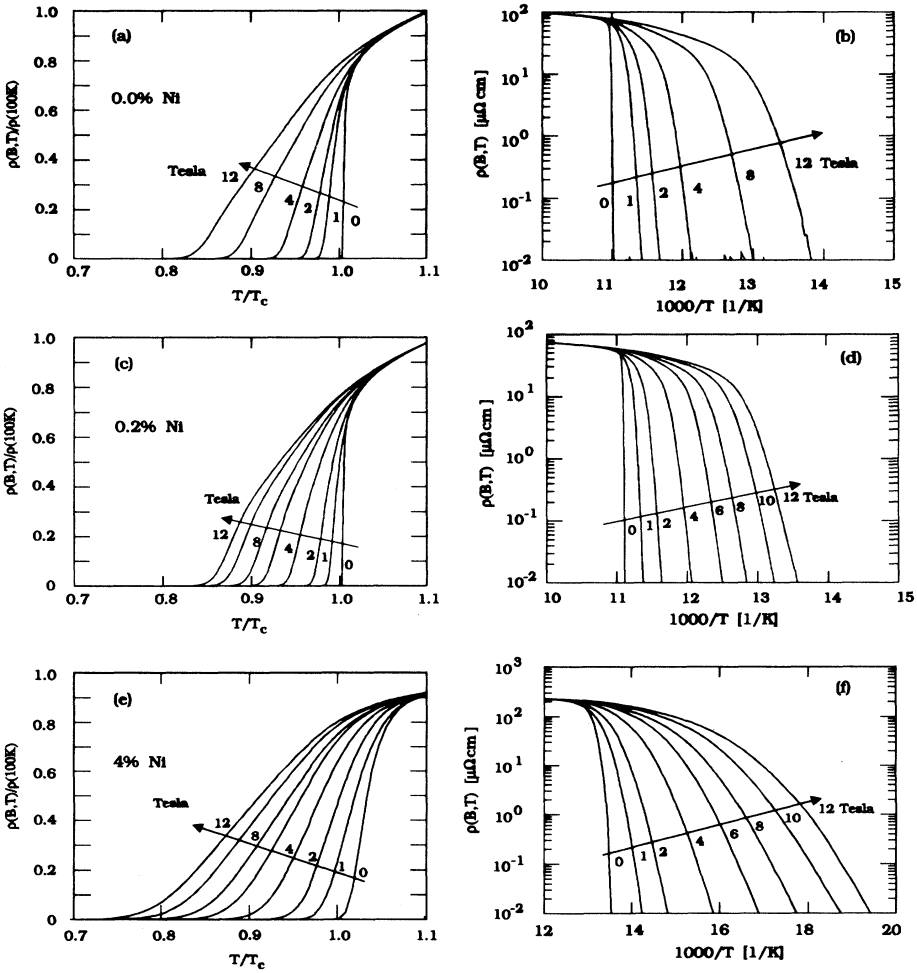

FIG. 3. Examples of the broadening of the resistive transitions to superconductivity for different magnetic fields for Ni concentrations of 0% (a), (b), 0.2% (c), (d), and 4% (e), (f). The left column shows the normalized resisitivity $\rho(T,B)/\rho(100\,\mathrm{K},B)$ vs reduced temperature T/T_c. Arrhenius plots of the same data are shown in the right column. The broadening in magnetic field of a slightly doped film (0.2% Ni) is smaller than those of an undoped or a highly doped specimen.

$$C_C = \begin{cases} 0, & x < 4\%, \\ \beta(x-4), & x \geq 4\%. \end{cases} \quad (4)$$

The Ni concentration on the plane sites C_P is determined by the boundary condition $C_P + C_C = x$. The fit parameters were $\tilde{\rho}_{C0} = 723\,\mu\Omega\,\mathrm{cm}$, $m_C = 4276\,\mu\Omega\,\mathrm{cm}/(\mathrm{at.}\,\%\ \mathrm{Ni}$ in chains), $\rho_{P0} = 299\,\mu\Omega\,\mathrm{cm}$, $m_P = 226\,\mu\Omega\,\mathrm{cm}/(\mathrm{at.}\,\%\ \mathrm{Ni}$ in planes), and $\beta = 7\%$. These values lead to a ρ_a/ρ_b ratio for undoped films of 1.58 in agreement with the results of Welp *et al.*, who find values between 1.2 and 1.85. But one must not conclude that β is the exact fraction of Ni occupying the chain sites at higher values, since inserted values for β up to $\beta = 33.3\%$ also lead to fit values consistent with Welp *et al.* with hardly visible deviations from the best-fit curve.

IV. Ni-INDUCED PINNING EFFECTS

The broadening of the resistive transitions in fields up to 12 T parallel to the c axis of the films was also investigated in terms of thermally activated flux flow. Figure 3 gives a survey of these transitions for different doping concentrations both in linear and in Arrhenius plots. Since the broadening in magnetic field has its lowest value for $x = 0.2$ at. % Ni (even lower than for the undoped films), these are first indications of the pinning effectiveness of the Ni dopants. Based on discussions by Palstra *et al.*[10] and Tinkham[11] a temperature dependence

$$U_c(t) = U_c(0)(1-t^2)^2\left(\frac{1+t^2}{1-t^2}\right)^{0.5} \quad (5)$$

of the activation energy was fitted to the resistive data using a field-dependent $t = T/T^*(B)$, where $T^*(B)$ is the temperature of the maximum in the slope $d\rho/dT$. In Fig. 4 this experimentally deduced activation energy

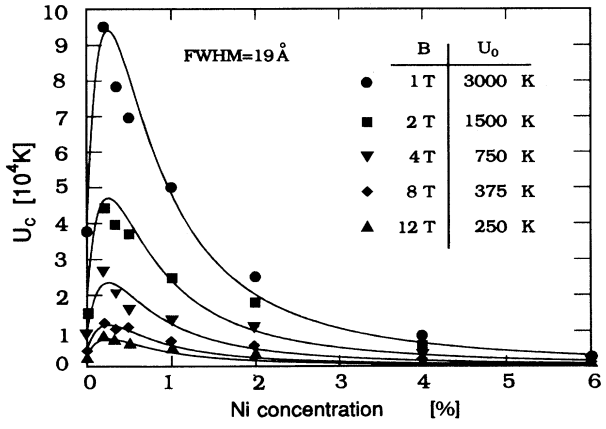

FIG. 4. Mean activation energy U_C vs Ni content for different magnetic fields. High values of U_C correspond to low broadenings of transitions in magnetic fields. The sharp maximum for U_C at $x \approx 0.2\%$ indicates the pinning effectiveness of Ni. The solid lines are fits to the activation energy according to a model of Schmitt *et al.* (Ref. 12) using the fit parameters U_0 as shown in the inset. Details are given in the text.

U_c for the movement of a correlated length of a vortex (about 500 Å) is plotted versus the Ni concentration. For x below 1% the values are higher than those of undoped films, indicating additional pinning due to the Ni atoms.

A model proposed by Schmitt *et al.*[12] is able to explain the dependence of $U_c(0,x)$ qualitatively: For small concentrations x the number of independent pointlike pinning centers along the correlated length of a flux line increases linearly with x. Therefore, the activation energy for thermally activated flux movement also increases with x. For higher concentrations the local pinning potentials begin to overlap. In this way the effective potential barrier for the flux movement is reduced, leading to the observed decrease in $U_c(0,x)$ for $x > 0.3\%$. The fit functions in Fig. 4 were calculated using a Gaussian-shaped pinning potential with a FWHM value of 19 Å. The inserted table shows the fit parameters U_0 used to obtain the plotted fit curves. These values describe the depth of the local pinning potential $U(r)$ of a single impurity atom.

The additional pinning due to the Ni doping is also obvious in measurements of the critical-current density j_c. Figure 5 shows the critical-current density versus magnetic field for slightly doped films at 77 K and at 4.2 K. Without magnetic field undoped films of different origin

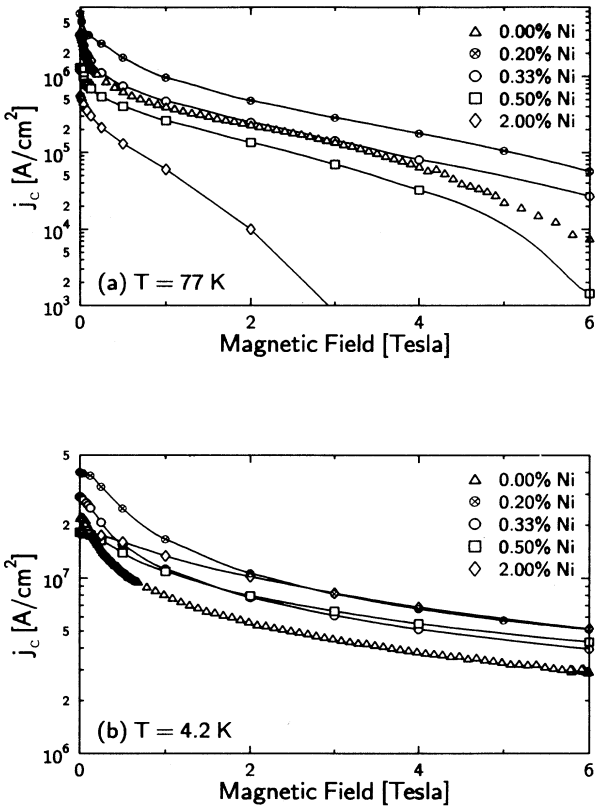

FIG. 5. Critical-current density $j_c(B)$ for five samples of different Ni concentration at 77 K (a) and 4.2 K (b). Slightly doped films have up to 8 times higher j_c values at 77 K and 6 T than an undoped sample indicated by triangles.

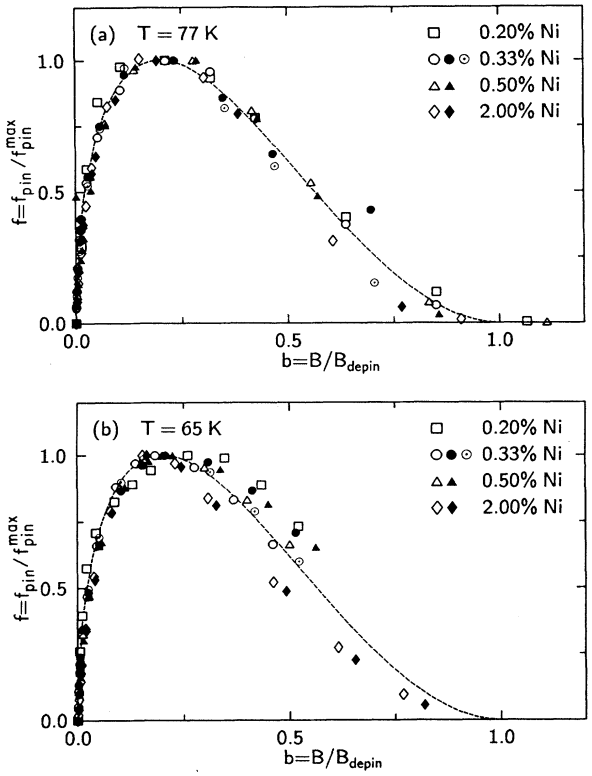

FIG. 6. Normalized pinning-force density f_p vs reduced field $b = B/B_{\rm depin}$ at 77 K (a) and 65 K (b) for eight films of different Ni concentrations. The depinning criterion was $B_{\rm depin} = B\ [\rho = 0.1\%\rho(100\,{\rm K})]$. A pinning function $f_p \propto \sqrt{b}(1-b)^2$ proposed by Kramer (Ref. 15) is plotted as a dashed line fitting the experimental values.

show j_c values between 2 and 4×10^6 A/cm^2 at 77 K, while $YBa_2(Cu_{1-x}Ni_x)_3O_{7-\delta}$ with $x = 0.2\%$ carries a critical current of about 6×10^6 A/cm^2. In high magnetic fields the j_c values decrease less than those of undoped films, leading to up to 8 times larger critical-current densities at 6 T than those for undoped samples, which is further evidence of the pinning effectiveness of Ni.

From experiments with classical superconductors, it is known that the pinning-force density defined as $f_p = |\mathbf{j}_c \times \mathbf{B}|$ obeys scaling laws of the form $f_p \propto [B_{c2}(T)]^n f(b)$ with n found to be $n = 2$ (Ref. 13) or $n = 2.5$.[14] The $YBa_2(Cu_{1-x}Ni_x)_3O_{7-\delta}$ films presented here show a scaling with $n = 1.6-2.2$ deduced from a double logarithmic plot of $f_{p,\rm max}$ versus $B_{\rm depin} = B\ [\rho = 0.1\%\rho(100\ {\rm K})]$. This exponent is not clearly correlated with the Ni content. As can be seen in Fig. 6, the reduced pinning force density scales with $f_p/f_{p,\ \rm max} \propto \sqrt{b}(1-b)^2$ in agreement with a scaling proposed by Kramer.[15]

V. HALL EFFECT, MOBILITY, AND HALL ANGLE

Figure 7(a) shows the Hall concentration $n_H = 1/R_H e$ and the Hall number $n_H V_{\rm uc}$ for $YBa_2(Cu_{1-x}Ni_x)_3O_{7-\delta}$ films of different doping levels, with $V_{\rm uc}0 = 175$ Å^3 being the volume of a unit cell. A slight increase for small doping levels is visible up to approximately 2% followed by a reduction both of n_H and dn_H/dT for higher Ni concentrations. The slope dn_H/dT at $x = 15\%$ is reduced to about half the value of undoped films, which indicates the already known correlation of T_c with dn_H/dT.[16] The interesting peak in $n_H(x)$, which is plotted in Fig. 7(b), possibly shows an increase of the carrier concentration and was also reported but not discussed by Clayhold, Ong, and Wang[16] with the only difference that in our measurement the peak occurs at $x = 0.5\%$ in contrast to $x = 2\%$ in the investigation of Clayhold, Ong, and Wang. They also studied the variation of the Hall number and the slope dn_H/dT at different Ni concentrations and found that the temperature dependence of n_H is related to the value of T_c, both vanishing at the same doping level. Szunyogh, Weinberger, and Podloucky[17] proposed a different variation of the density of states at the Fermi level, $N(E_F)$, of $YBa_2(Cu_{1-x}Ni_x)_3O_{7-\delta}$ depending on the site preference of Ni. Their calculations show an increase of $N(E_F)$ for Ni substitution in planes and a decrease for substitution in chains. Another possible explanation worth discussing is based on the assumption of $YBa_2Cu_3O_{7-\delta}$ being an entropy-stabilized com-

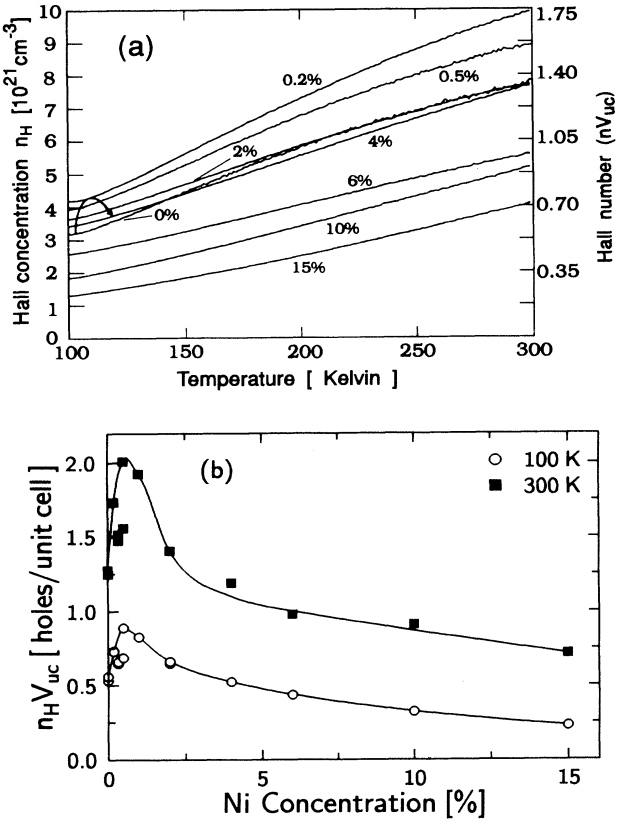

FIG. 7. Temperature dependence of the Hall concentration n_H for different doping levels $0 \le x \le 15\%$ (a). The absolute value n_H and also the slope dn_H/dT decrease with Ni concentration $x \gtrsim 3\%$, whereas for lower Ni content both increase with increasing x. In the lower plot (b) this concentration-dependent peak effect in $n_H V_{\rm uc}(x)$ with a maximum at $x \approx 0.5\%$ is shown for 300 K and 100 K (the solid lines are guides to the eye).

pound. In such compounds (e.g., $CuFe_2O_4$, Fe_2TiO_3) the enthalpy H is positive (i.e., compound formation is endotherm; see, for example, Ref. 18) while the Gibbs potential $G = H - TS$ must be negative. Therefore, in entropy-stabilized compounds, the second term TS must be large enough to compensate H either by a high degree of disorder or by high temperature, explaining why such compounds are only metastable at low temperatures. There are some indications that high-temperature superconductors are entropy stabilized,[19] which leads us to favor the following picture: In pure $YBa_2Cu_3O_{7-\delta}$, oxygen deficiency is a source of entropy, stabilizing the system and leading to a stoichiometry with $\delta \geq 0$. Substituting Ni for Cu generates an increase of entropy such that δ can be smaller while the system is still stable. Hence the Hall number, which is proportional to the carrier concentration, increases with decreasing oxygen deficiency.

While the Hall concentration shows this interesting behavior, the mobility $\mu = R_H/\rho$ as shown in Fig. 8 does not. With increasing Ni content μ decreases monotonically, showing an obstruction of carrier hopping that is slightly greater at low x than at higher Ni concentrations. Despite the scatter of the data $\mu(x)$ as plotted for $T = 100\,\mathrm{K}$ (b) and $T = 300\,\mathrm{K}$ (c) appears to decrease significantly more rapidly below $x \leq 4\%$ and less rapidly at higher concentrations. This is another indication of the site preference model discussed in the resistivity section.

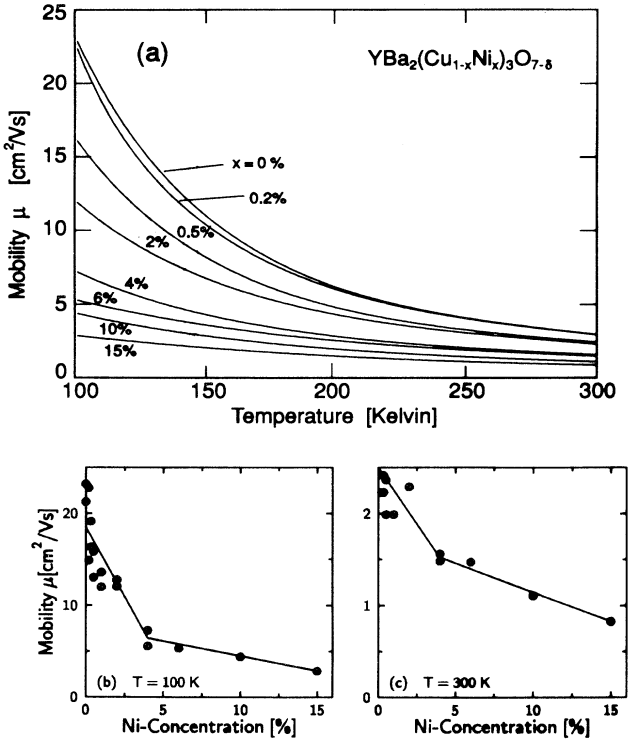

FIG. 8. Mobility μ vs temperature for different $YBa_2(Cu_{1-x}Ni_x)_3O_{7-\delta}$ films (a). Contrary to the Hall concentration n_H, μ decreases monotonically with increasing x, which is displayed here for 100 K (b) and 300 K (c). Solid lines should guide the eye.

The dependence of the cotangent of the Hall angle $\cot\Theta_H = 1/\mu B = \sigma_{xx}/\sigma_{xy}$ on the Ni concentration is a powerful instrument to investigate the nature of the temperature dependence of the Hall coefficient. Since the classical explanations for obtaining a temperature dependence of $R_H \propto 1/T$, i.e., multiband models or the skew-skattering model fail to explain the observed behavior of Hall data entirely, new models have been proposed. One of these theories is the resonating valence bond (RVB) model of Anderson.[20]

Since the RVB model predicts the transport conductivity to be proportional to the transport relaxation time ($\sigma_{xx} \propto \tau_{\mathrm{tr}}$) and the Hall resisitvity to be proportional to the product of transport and Hall relaxation time ($\sigma_{xy} \propto \tau_{\mathrm{tr}}\tau_H$), the Hall angle allows the measurement of the Hall relaxation time and a test of this model. According to Anderson

$$1/\tau_H = T^2/W_s + 1/\tau_M, \tag{6}$$

which leads to

$$\cot\Theta_H = \alpha T^2 + C(x), \tag{7}$$

where $C(x)$ is a (linear) contribution of impurities. α should be independent of the doping level because it in-

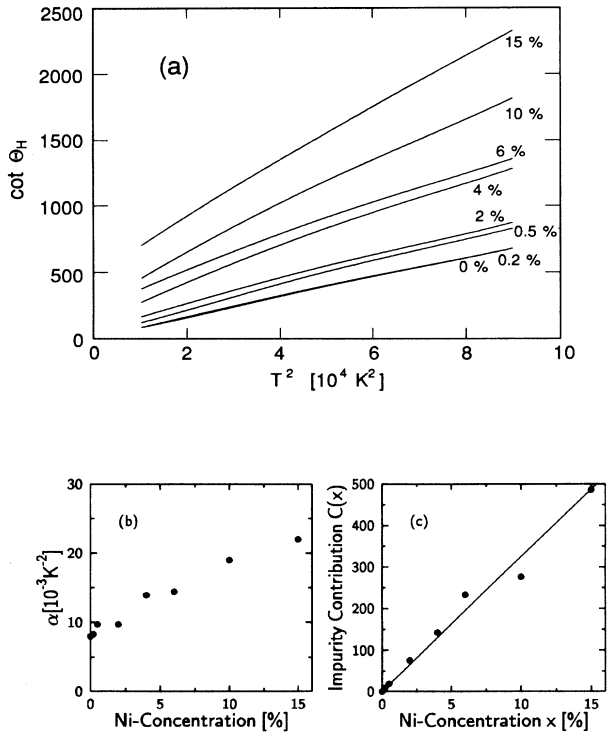

FIG. 9. Cotangents of the Hall angle $\cot\Theta_H$ for different doping concentrations are plotted vs T^2 as a test of the RVB model (Ref. 20) (a). The dependence of the slope α of the curves on the Ni concentration (b) disagrees with experiments of Chien, Wang, and Ong (Ref. 21) and does not confirm the prediction by the RVB theory, whereas the impurity contribution $C(x)$ to $\cot\Theta_H$ is linear in Ni concentration with $C(x) = 32x/(\mathrm{at.}\,\%\ \mathrm{Ni})$ (c), as would be expected in the RVB theory.

dicates the bandwidth of spin excitations W_s in the CuO_2 planes. Chien, Wang, and Ong[21] tested the RVB model using a series of Zn-doped $YBa_2Cu_3O_{7-\delta}$-single crystals with $0\% \leq x \leq 5\%$. While Chien, Wang and Ong confirmed Anderson's predictions by plotting $\cot\Theta_H$ versus T^2 for $0\% \leq x \leq 3.5\%$, we did not find the same behavior for our epitaxial $YBa_2(Cu_{1-x}Ni_x)_3O_{7-\delta}$-films. As can be seen from Fig. 9(a), the slope and hence α are not independent of the doping level, showing an increase of this value especially at concentrations higher than $x = 2\%$ The measured values of α range from $8 \times 10^{-3}/K^2$ to $22 \times 10^{-3}/K^2$ (b), leading to W_s values between 901 and 544 K. Nevertheless, $C(x) = \beta x$ shows a linear dependence on the Ni concentration with $\beta = 32/(\text{at.}\,\%\ \text{Ni})$ as displayed in Fig. 9(c).

VI. CONCLUSIONS

A series of high-quality $YBa_2(Cu_{1-x}Ni_x)_3O_{7-\delta}$ films has been prepared by high-pressure oxygen sputtering. No impurity phases were detected. A change in slope of $T_c(x)$ and $\rho(x)$ could be explained consistently by a model of different site preference of the Ni atoms depending on the Ni concentration. Fits of $\rho(x)$ treating $YBa_2Cu_3O_{7-\delta}$ as a parallel circuit of the CuO chains and the CuO_2 planes lead to values of ρ_a/ρ_b consistent with those reported by Welp *et al.*[9] The increase of the activation energy and of the critical-current density for small doping concentrations shows the pinning effectiveness of the dopant. The pinning-force density scales with $\sqrt{b}(1-b)^2$ as proposed by Kramer.[15] The carrier density n shows a slight increase for small x values as already reported but not discussed by Clayhold, Ong, and Wang.[16] Nevertheless, the mobility μ decreases monotonically with increasing Ni content. Investigations of the Hall angle Θ_H were not able to confirm all of the predicted behavior of Anderson's RVB model.[20]

ACKNOWLEDGMENTS

The authors acknowledge financial support by the Bundesminister für Forschung und Technologie and the Deutsche Forschungsgemeinschaft through SFB 252. One of us (C.T.-R.) was supported financially by the Conselho Nacional de Desenvolvimento Cientifico e Technológico do Brasil–CNPq.

[1] T. Kajitani, K. Kusaba, M. Kikuchi, Y. Syono, and S. Nielsen, Jpn. J. Appl. Phys. **27**, L354 (1988).
[2] K. Westerhold, H. J. Wüller, H. Bach, and P. Stauche, Phys. Rev. B **39**, 11680 (1989).
[3] H. Shaked, J. Faber, Jr., B. W. Veal, R. L. Hitterman, and A. P. Paulikas, Solid State Commun. **75**, 445 (1990).
[4] J. F. Bringley, T. M. Chen, B. A. Averill, K. M. Wong, and S. J. Poon, Phys. Rev. B **37**, 5932 (1988).
[5] R. S. Howland, T. H. Geballe, S. S. Laderman, A. Fischer-Colbrie, M. Scott, J. M. Tarascon, and P. Barboux, Phys. Rev. B **39**, 9017 (1989).
[6] J. B. Boyce, F. Bridges, T. Claeson, T. H. Geballe, and J. M. Tarascon, Supercond. Sci. Technol. **4**, 343 (1991).
[7] N. Peng, J. Yuan, D. Zheng, and W. Y. Liang, Supercond. Sci. Technol. **4**, 313 (1991).
[8] C. Tomé-Rosa, G. Jakob, M. Maul, A. Walkenhorst, M. Schmitt, P. Wagner, P. Przysłupski, and H. Adrian, Physica C **171**, 231 (1990).
[9] U. Welp, S. Flesher, W. K. Kwok, J. Downey, Y. Fang, G. W. Crabtree, and J. Z. Liu, Phys. Rev. B **42**, 16 (1990).
[10] T. T. M. Palstra, B. Batlogg, R. B. van Dover, L. F. Schneemeyer, and J. V. Waszczak, Phys. Rev. B **41**, 6621 (1990).
[11] M. Tinkham, Phys. Rev. Lett. **61**, 1658 (1988).
[12] M. Schmitt, A. Walkenhorst, C. Tomé-Rosa, M. Paulson, P. Wagner, Th. Kluge, G. Jakob, and H. Adrian, in *Critical Current Limitations in High Temperature Superconductors*, edited by M. Baran, W. Gorzkowski, and H. Szyurczak (World Scientific, Singapore, 1992), p. 360.
[13] W. A. Fietz and W. W. Webb, Phys. Rev. **178**, 657 (1969).
[14] T. R. Haller and B. C. Belanger, IEEE Trans. Nucl. Sci. **NS-18**, 671 (1971).
[15] E. J. Kramer, J. Appl. Phys. **44**, 1360 (1973).
[16] J. Clayhold, N. P. Ong, and Z. Z. Wang, Phys. Rev. B **39**, 7324 (1989).
[17] L. Szunyogh, P. Weinberger, and R. Podloucky, Phys. Rev. B **43**, 519 (1991).
[18] A. Navrotsky, in *Solid State Chemistry*, edited by A. K. Cheetham and P. Day (Clarendon, Oxford, 1988), p. 382.
[19] A. W. Sleight, Physica C **162–164**, 3 (1989).
[20] P. W. Anderson, Phys. Rev. Lett. **67**, 2092 (1991).
[21] T. R. Chien, Z. Z. Wang, and N. P. Ong, Phys. Rev. Lett. **67**, 2088 (1991).